Temperature Evolution of Large-Scale Oscillating Heat Pipe with Methanol as the Working Fluid

Adi Winarta[1]
Mechanical Engineering Department
Bali State Polytechnic
Bali, Indonesia
[1]adi.winarta@pnb.ac.id

Nandy Putra[2], Raldi Artono Koestoer[3], Agus S. Pamitran[4]
Mechanical Engineering Department
Universitas Indonesia
Depok, Indonesia
[2]nandyputra@eng.ui.ac.id

Abstract—**As a family of heat pipe, oscillating heat pipe (OHP) has many additional unique operating parameters. This paper examined the characteristic of temperature evolution from start-up until dry-out stage of an OHP with extra-long dimension using methanol as the working fluid. The temperature evolutions were studied in the range of adjustable heater load from 20 Watts up to 467 Watts. The temperature evolution associated with flow pattern in two-phase regime as follows: chaotic intermittent slug flow, switch and reversed flow, transition to annular flow and stable circulation and dry-out stage. The lowest thermal resistance was 0.057 °C/W at 410 Watts. At the switch/reversed flow stage, the evaporator temperatures were separated into a certain level, which was a proof of net circulation flow**

Keywords—*Oscillating heat pipe, temperature evolution, methanol, dry-out*

I. INTRODUCTION

Heat pipe technology was one of the challenging fields in heat transfer application engineering. Oscillating Heat Pipe (OHP) has become one of the popular "heat pipe" research topics since being discovered by Akachi at early 1990 [1]. Although, there are still many fundamental questions regarding OHP, which still unanswered until now.

The OHP is built from a bent-capillary tube to form a meandering tube and partially injected with working fluid. Then, naturally the working fluid will form a train of liquid slugs and vapor plugs inside. The OHP structure consists of three parts, evaporator, adiabatic, and condenser sections. Evaporator and condenser sections are the places where heat transfer occurs. The evaporator absorbs heat from an object, which is then transferred to the condenser by the motion of the working fluid and rejects it to the heatsink. When the evaporator is in contact with thermal load, the working fluid inside will evaporate and then increases the local vapor pressure. The formation of bubbles will expand and move towards the condenser section. At this section the hot slug from the evaporator will collapse and condense due to the low saturation temperature and pressure. The growth and collapse of bubbles in the two sections lead to oscillating or pulsating motions within the tube. As a result of the pressure imbalance inside the OHP tube, the oscillation of working fluid will occur and transport heat from the evaporator to the condenser. These motions of working fluid will continue as long as the pressure difference exists. The flow of this working fluid undergoes both complex oscillatory displacements and

circulatory characteristics [2]. Ma stated that the OHP motion is a mechanical vibration system with a vapor plug acting as a constant spring [3]. Contrary to conventional heat pipes, OHP has a wickless structure inside. The wickless structure significantly reduces its weight, making it applicable for avionics and extra-terrestrial applications.

II. RELATED RESEARCH

Tseng et al.[4] investigated the performance of OHP with a capillary tube of 2.4 mm diameter. They used distilled water, methanol, and HFE-7100 as the OHP working fluid. They showed that the oval shaped tube provides lower heat start-up than the circular one. Cui et al. [5] studied OHP with distilled water, methanol, acetone, and ethanol as working fluids. They found that a dry-out appeared locally on some individual pipes in the evaporator. Elevating the power supply will cause the dry-out to spread to several other sections. Liu et al.[6] studied a start-up working fluid model consisted of ethanol, distilled water, methanol, and acetone. Their results showed that filling ratio, inclination, heat load, and properties of the working fluid strongly affected performance of the start-up. Naik et al.[7] examined acetone, methanol, and ethanol as working fluids at various filling ratios. They found out that acetone with 60% filling ratio had the lowest thermal resistance and the highest heat transfer coefficient. Verma et al.[8] demonstrated that methanol worked efficiently in a variety of orientations compared with distilled water. Tong et al. [2] conducted a study of OHP visualization with methanol as the working fluid. The visual study showed high amplitude of oscillation during the start-up stage. Xu et al. [9] observed the difference of advancing and receding angles of water when travelling inside the channel due to high surface tension. They also discovered bubble displacement of methanol oscillation versus time as the quasi-sine waves. Water OHP had periodic "stationary–fast movement" behavior of oscillation motion. An experimental study by Saha et al.[10] showed that methanol and water should be the first consideration when choosing a working fluid for open loop OHP with vertical and horizontal orientation. Several visual studies have been conducted by various researchers that successfully characterized at least five different flow patterns [2, 9, 11-16]. The results were dispersed bubble, vapor plug, long vapor plug, semi-annular flow and annular flow. Khandekar and Groll also conclude that the occurrence of different flow patterns is due to the increasing function of the heat input level[17].

Studies of the characteristics of long OHP are notably rare. This scarcity makes sense because OHP was originally developed to provide thermal management solutions for small electronic devices. Especially electronic devices which have strict requirements for space limitations and high heat flux rejection. Some applications of long OHP have been tested and reported [18]. Xian et al.[19] tested OHP with evaporator length of 200 mm with water and ethanol as working fluids. They found that the maximum thermal conductivity for water peaks at 295 kW/mK, and for ethanol at 111 kW/mK. There is a potential for high thermal transfer capability over long distances using large scale of OHP design.

Based on this, the objective of this research is to study the characteristic of temperature evolution from start-up to the dry-out stage of large scale OHP using methanol as the working fluid. Thermal performance of OHP strongly depends on the temperature characteristics of evolution on the evaporator and condenser, which are also strongly influenced by the physical properties of the working fluid.

The schematic of the experimental facility shown in Fig. 1 consists of a long multi-turn OHP, electrical heating system, a water cooling system, and data acquisition system. The OHP is made of a copper capillary tube with inlet and outlet diameter of 1.6 mm and 3.0 mm with18 meandering turns. The evaporator, adiabatic, and condenser are of 200, 280, and 240 mm. The overall dimension of OHP is 760×400 mm and the total OHP length is 13.6 m.

To explore the effect of different heat input levels, Ni-Cr wire heater was attached at evaporator section. Heat supply was measured and regulated using power meter (Yokogawa WT310 with error measurement $\pm$ 0.01%) and voltage regulator. The condenser section placed inside an acrylic cooling box, which had an inlet and outlet to circulate cold water. The temperature of the cold water supplied to the condenser cooling box was constant at 25°C (error ±0.5°C) by using thermostatic bath. The flow rate of the cold-water supply was constantly regulated at 6 gram/sec by using rotameter ®Platon. Temperature were measured using thermocouple type K (error $\pm$ 0.3 °C), which connected to data acquisition system (NI-9174, NI 9213 and LabVIEW). Evaporator and adiabatic sections were insulated with glass wool and polyurethane to prevent heat loss to the ambient.

III. RESEARCH METHODOLOGY

Filling ratio is the ratio of the liquid volume to the total volume of the OHP capillary tube. Data collection began after the evaporator, adiabatic, and condenser temperature stabilized at 25 °C (±0.7 °C). The experimental parameters in these tests were the evaporator and condenser temperatures versus the supplied heating power. The power level during the test started at 20, 30, 40, 50 W until permanent dry-out occurred at the evaporator. Thermal resistance was calculated in the last 10 minutes of each power level to ensure oscillations were achieved in a steady state [9].
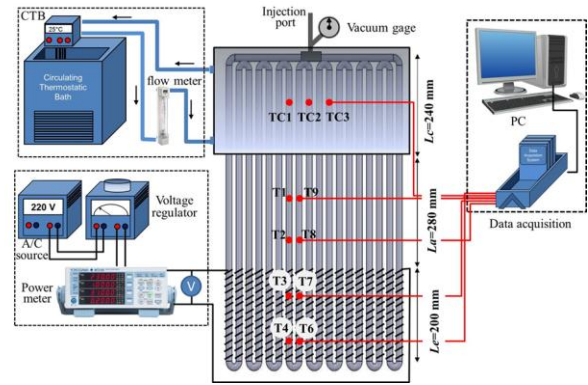

Fig. 1. Schematic experimental test for long OHP

Although quite simple, thermal resistance is a convenient method to analyses the thermal performance of a heat pipe and can be obtained by equation (1) as follow;

$$R_{th} = \frac{T_e - T_c}{Q} \qquad (1)$$

where R_{th} is the thermal resistance, Q is the thermal power supplied from a Ni-Chrome wire heater measured by a power meter, T_e is the average temperature at evaporator and T_c is the average temperature at condenser.
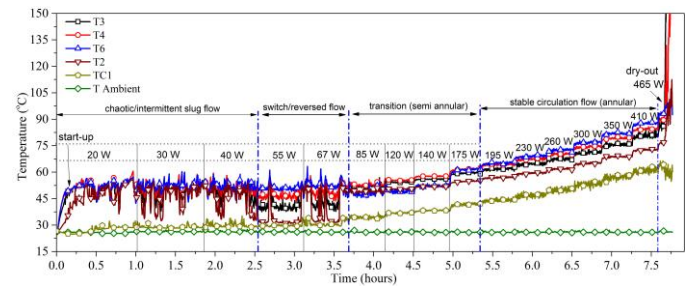
IV. RESULT AND DISCUSSION

Fig. 2 The whole temperature evolution from start-up at 20 Watt until dry-out happened at 467 Watt.

One of the methods to evaluate OHP characteristics and performance is by observing the oscillation temperature of the evaporator, adiabatic and condenser. The observations of temperature evolution were analyzed and associated with visualization studies by previous researchers [2, 9, 12, 15, 20]. Fig. 2 shows the results of the temperature evolution of the long OHP with methanol working fluid. Each heat input was marked on the time series line; expanded views of each stage are discussed in the next sections.

4.1 Random/chaotic slug flow at low heat input

4.1.1 Initial heat input (20 Watts)

When heat was applied on the evaporator section, the evaporator temperature (T4) and adiabatic (T2 and T8) immediately increased with different degrees of slope (shown in Fig. 3a). This difference was attributable to the variation in distance of the evaporator and adiabatic from the heat source supplied by the wire heater. Conduction heat transfer occurred through the capillary pipe wall, liquid slug and thin film layer

which surround the vapor plugs. Before sufficient temperature gradient was occurred between evaporator and condenser, there was no macro movement of liquid and vapor plug inside the channel. The heat supply only increased the temperature of evaporator wall and working fluid. After approximately 200 seconds, temperatures at T8 and T4 up and down, respectively; due to the movement of liquid and vapor plug. The formation of liquid and vapor slug would be pushed upwards by bubble expansion (start-up condition, see Fig. 3a). Very unstable oscillation at the evaporator and adiabatic was result of intermittent bubble expansion. Boiled free convection generated dispersed bubbles at low heat flux (as shown Fig. 3b, zone I). These dispersed bubbles created by the nucleation sites at the pipe surface moved upwards immediately and later collapsed due to condensation at the adiabatic. Temperature spikes (T2 and T8) were proof of the existence of two-phase heat transfer from collapsing bubbles (at zone I). Continuous cooling continued occurred at the condenser section (zone I), because of the slow movement of working fluid inside. Reduction of movement of the working fluid at the condenser occurred because of flow resistance from the long surface wall inside the capillary tube. As heat input was continuously applied to the evaporator, more dispersed bubbles should be generated from nucleate boiling (zone II). A number of dispersed bubbles might coalesce with each other to form a larger bubble. Fig. 3b illustrates bubble coalescence from visualization study references [5]. More active temperature oscillations can be seen in the adiabatic section. An anti-phase temperature shown at zone II indicates up and down motion of working fluid due to balancing force at neighboring channels.
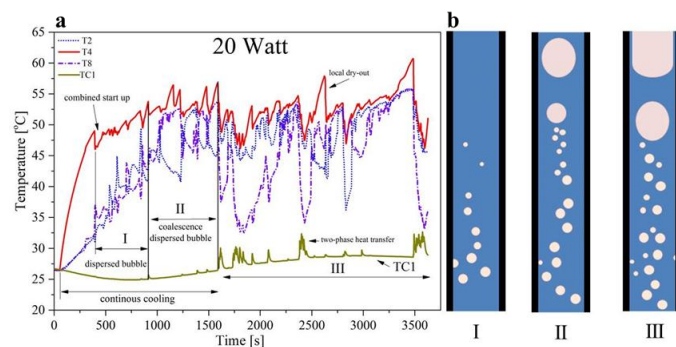

Fig. 3 (a) Temperature evaporator and condenser at heat supplied of 20 Watts (b) Prediction illustration for start-up region.

The condenser temperature began to oscillate after period of time as a result of the hot slug reaching the condenser deeper than before (Zone III). Temperature spikes indicated that these hot slugs fully collapsed inside the condenser sections (TC1). Soon, temperature oscillation with higher amplitude occurred in the evaporator, adiabatic and condenser. As stated by Senjaya and Inoue, a large driving force would only occur at TS bubble formation [14]. TS bubble has a large driving force to push the arrangement of liquid-vapor upward; therefore, bulk circulation flow occurs inside the channel and enhances heat transport from the evaporator to the condenser section.

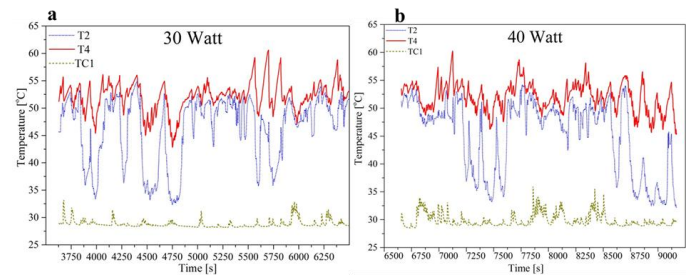### 4.1.2 Heat input at 30 Watts and 40 Watts

Fig.4 a) Heat supply at 30 Watts and b) heat supply at 40 Watts

Fig. 4a shows the temperature evolution of heat supply at 30 Watts. Higher frequency and amplitude of temperature oscillation were resulted from the increased level of heat supply. Irregular fluctuations of temperature oscillation were occurred due to unusual of length effective of OHP. More heat requires to push the fluid upward thus proper heat transport can be established. Therefore, at low heat input stage (including 30 Watt), random and unstable temperature still exists. As reported by Xu et al., methanol has a characteristic of long vapor plug [13]. Thus, long vapor break-up in the condenser occurred due to incomplete condensation and quite possibly occur at this stage. more vapor bubble growth at nucleation sites, which in turn augment the driving force. The hot slugs are able to penetrate the condenser section deeper than previous heat supply. As a result, more vapor plug condensed in the adiabatic section. This will increase the average temperature at the condenser substantially. The vapors which are condensed to liquid slug have higher density and push the fluid to the bottom side. The gravity and fluid redistribution at the condenser also support the fluid motion down to the evaporator section. It is responsible for the redistribution of the liquid and vapor slug composition. Redistribution of fluid compositions results in alternating reversals of bulk motions of the working fluid. This unstable and unsteady temperature fluctuation at low heat input was generally characterized by slug flow mode [21]. However, higher mass transition due to higher frequency and amplitude of temperature oscillation effectively reduced the thermal resistance of the device as shown in Fig. 9.

The frequency of temperature oscillation at the evaporator was raised with slight decrease of amplitude after being increased to 40 Watts heat supplied. The temperature spikes also became sharper and faster as shown at Fig. 4b. At this stage, local oscillations with low amplitude are superimposed with the main temperature wave. Short vapor plugs which have larger buoyancy force than the long ones, will push the upper liquid, which presses the vapor down due to gravitational force [9]. Sharp increase and decrease in temperature at the evaporator and adiabatic had shorter periods than the previous heat input. In addition, temperature oscillation at the adiabatic has more active motion. Higher amplitude and frequency of temperature fluctuation at the condenser also increased, indicating more vapor fully condensed at this stage. According to the visualization study [12], the random movement of working fluid at low heat supply resulted from slug flow of bulk circulation flow. The more active slug flow bulk circulation is, the higher heat transfer coefficient of force convection is and the lower the thermal resistance is. This is in line with Mameli experiment that

large amplitude would result in large coefficient of forced convection[21]. Sharp decrease of thermal resistance occurred at this stage. Overall, the temperature still could not reach the steady state, and no net circulation was found at this stage.

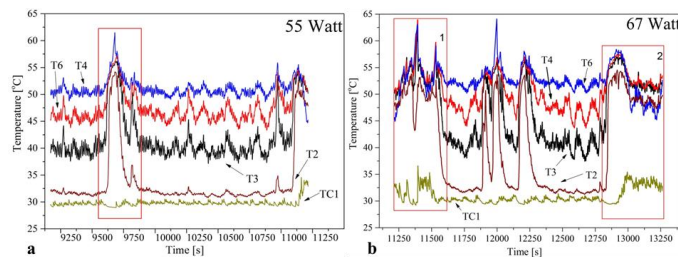### 4.2 Intermittent and switch flow at quasi steady circulation

Fig.5 Heat supply at 55 Watts (a) and 67 Watts (b)

Increasing the level of heat supply to 55 Watts leads to an increase in the frequency of oscillation but decreases the amplitude of oscillation. The evaporator temperature also separated into some levels, which are not found at previous heat inputs (as shown at Fig.5). These might be indicated that higher velocity of fluid motion was generated from a larger driving force. Higher driving force is able to generate one-way circulation. High pressure at the evaporator was sufficiently enough to generate circulation flow which makes the fluid motion through the condenser section. And then reaches the adjacent tube. Higher heat supply along the evaporator section results in increase of the evaporation rate of liquid slug. The amount of mass influx increases the mass quality of the working fluid which then results in flow pattern change. During circulation flow, the liquid slug oscillates axially but in lower frequency than the previous heat supply. This "oscillatory circulation" also was reported recently by Borkar and Pachghare [12]. The separation level of evaporator temperatures seems evidence of circulatory oscillation of the working fluid inside the OHP in addition to the visualization studies. Previous visualization studies [17, 18] also showed that slug flow pattern would show higher amplitude of temperature oscillation than annular flow. It seems that, TC1−T2, which is a down-comer flow, is a slug flow pattern and up-comer motion from T6−T7 which is a semi-annular flow.

Even though the circulation flows already occur at 55 Watts, the stability of the motion has not been reached. The red box at Fig. 5a shows a sudden increase of evaporator temperature which is then followed by other temperature sections. This occurred because of a stop-over of fluid flow which is a consequence of local dry-out at the evaporator section. These phenomena rarely occur at standard multi-turn OHP[17]. Due to the long dimension of OHP, stop-over occurs frequently. This stop-over motion is also responsible for reversed direction flow at this heat supply. Changes in condensation rate, vapor coalescence and nucleate boiling are the reasons for stop-over and reverse motions of working fluid[22, 23]. If there is a change of condensation rate at one of the two sides of the condenser section, the direction of working fluid circulation will follow the highest rate of condensation [20].

Further increase of heat supply to 67 Watts (Fig. 5b) might lead to new instability of evaporator and adiabatic temperature

fluctuations. As shown at the first red box, a short period of sharply increased and drop evaporator temperature occurred at evaporator sections. The fluid oscillations were stagnant if the temperature of the evaporator increases. After a short time, the viable fluid motion begins again. At the second box (Fig. 5b), the stagnation occurs with a longer period and later breaks up after a certain time. It is found that the fluid still oscillates with low amplitude at the stagnation period. The circulation of working fluid then changes to reverse direction and stabilize until heat is supplied. At this heat supply, the fluid motion was poor after the separation of temperature was lost.

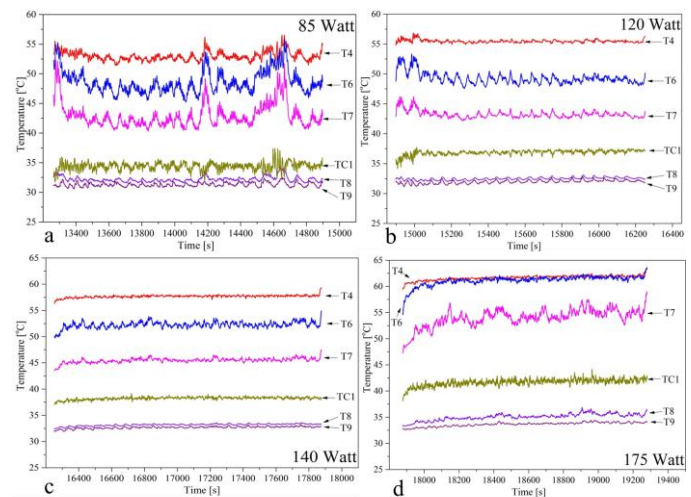### 4.3 Transition to stable motion circulation

Fig.6 Heat supply (a) 85 Watts, (b) 120 Watts, (c) 140 Watts and (d) 175 Watts

Fig. 6 shows the temperature evolution at transition stage due to the increments of heat supply. As heat increases from 85 to 140 Watts, the amplitude of temperature oscillations decreases gradually (Fig. 6a-c). The temperature T4 at 140 Watts oscillates with the lowest amplitude (Fig.6c). Increasing the heat supply will directly raise the evaporator temperature.

The temperature difference between evaporator and condenser at 85−140 Watts were relatively constant between 12−13 °C. It was increased (17°C) at higher heat supplied (175 Watt). Higher heat supply leads to higher temperature saturation and increased quality of vapor at the evaporator. Higher temperature saturation will evaporate more liquid film at the evaporator section. If more liquid film evaporates, more vapor bubbles will be generated and result in larger driving force. The motions of hot slug to the condenser would be faster. If the driving forces are sufficiently high, then the velocities of vapor plug would be sufficient to penetrate the liquid slug [24]. The liquid slug will break up, and the liquid will join the thin liquid film at wall surfaces. The two vapor plugs will merge forming a long vapor plug. If a few long vapor plugs join together due to the high velocity of vapor, a semi-annular flow pattern will exist at this stage. Higher heat flux also results in decreasing the surface tension of liquid slug (σ_{liq}). Higher velocity of vapor plugs eventually will change the flow pattern into semi-annular and then annular flow. The increase of heat supply does not decrease the amplitude of temperature oscillation as previously shown in Fig. 6a-c. Instead, increasing to 175 Watts results in higher amplitude (Fig. 6d). Longer cooling periods at the

condenser result in higher amplitude of temperature oscillation (as shown at Fig. 6d). This effect may result from the high velocity of vapor and high evaporation rate at higher heat supply. As stated by Borkar and Pachghare in their visualization study, there are four types of characterization at annular flow [12], which are classified as follows; churn, wispy, mist and pure annular flow. There is wavy liquid thin film in the first three of annular flow that will increase the amplitude of oscillation at 175. From visualization studies [12, 21], it seems that the flow pattern at this stage was in transition from semi-annular to annular flow.

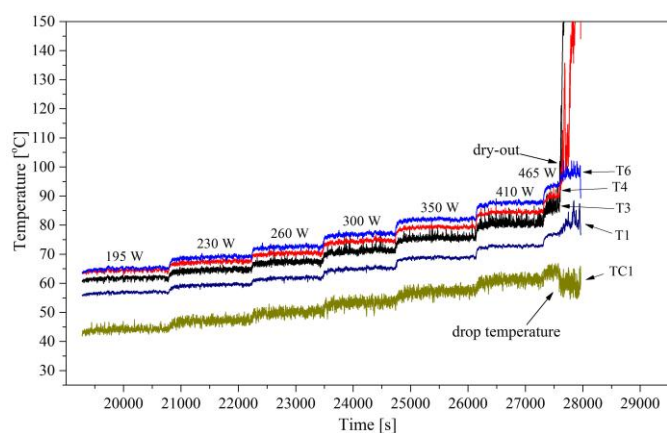### 4.4 Steady temperature and dry-out at evaporator

Fig. 7 Stable and steady temperature at heat supply from 195 to 400 Watts

Fig. 7 illustrated the temperatures evolution of OHP at heat supplied from 195 to 465 Watts. Steady temperature was shown this stage after the heat balance occurs. The initial critical power at 195 Watts starts sustainably stable net circulations. The higher speed of vapor plugs at the annular flow pattern results in a decrease of vapor growth generation time. This is the reason why the evaporator temperature difference is closer at this heat input. The amplitude of temperature fluctuations at the condenser was higher than at the evaporator section indicating that a higher coefficient of two-phase heat transfer occurs at the condenser. There was a step increase of average temperatures of the evaporator, adiabatic and condenser from the heat supply increments at the evaporator until 400 Watts. For each heat supply increment, there was a transient time of approximately 211 seconds until pseudo steady state is reached (as shown in Fig.8). In the transient stage, the temperature of the evaporator and condenser changing its thermal equilibrium state corresponds to the new temperature saturation. There might be a correlation between the new temperature saturation of each heat flux increment and the vapor mass quality of working fluid, which subsequently affect the amplitude of oscillation temperatures. The device is able to maintain the evaporator temperature below 95 °C until 400 Watts of heat supplied.

The evaporator temperature (T3 and T4) soars to more than 150°C after a certain time of 465 Watts heat supply (as shown in Fig. 7 at 475 Watts). Dry-out occurs at the device due to insufficient liquid supply at the evaporator section [22]. The device is no longer able to sustain net circulation flow. An enormous pressure jump of vapor plugs at dry-out spots retards

the circulation of working fluid and results in poor fluid motion. As a consequence, the supply of colder working fluid from the condenser will hold at the condenser, and continuous cooling will occur at the condenser. This will result in a drop of condenser temperature and the thermal resistance of the device will increase gradually.

This indicates that dry-out only occurs at some specific locations. This occurs due to the uneven distribution of heat flux from the wire heater. At dry-out spots (T6 and T7), the liquid thin film evaporates very quickly until no liquid is left inside the tube. After that the temperature of superheated vapor will be increased to the critical point where the device can experience burn-out conditions. This dry-out will create a high-pressure surge which then can block the flow of working fluid.
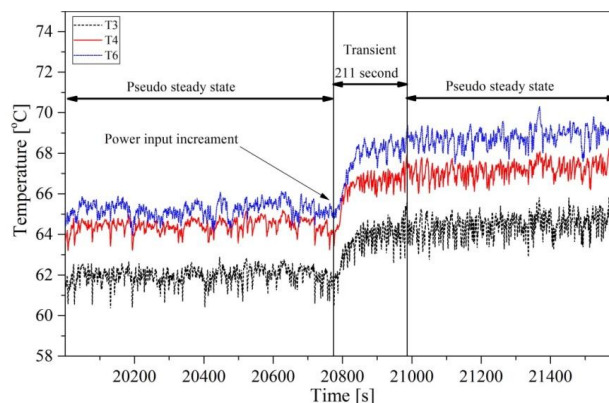

Fig. 8 Period of temperature transient between heat input 195 Watt to 230 Watt.

4.5 Overall thermal resistance

To discuss the relation between each stage of the temperature evolution with performance, the thermal resistance of each heat input was calculated using equation (1). Fig. 9 shows the thermal resistance of long OHP as a function of heat supply. At the start-up of the first stage, the thermal resistance drops significantly due to the movement of slug flow at start-up (1.16 °C/W to 0.73 °C/W at 20 to 30 Watts). The thermal resistance still exhibited a significant drop after further increase to 40 Watts. Due to significant sensible heat transfer at intermittent slug flow the thermal performance will drop significantly. At chaotic intermittent slug flow, the prominent heat transfer mode is forced convection of slug flow. This is shown by sharp decrease and increase of temperature oscillation in Fig.3 and Fig.4. The bubble growth and collapse at the evaporator and condenser mainly acts as the driving force of working fluid motion. At switch/reversed flow stage, the thermal resistance only slightly decreases at 55 to 67 Watts. This finding was observed as a consequence of no significant difference at both heat supplies in terms of flow motion. After the motion of working fluid reaches a net circulation, which appears at transition stage, thermal resistance begins to gradually decrease again. The decline of thermal resistance at the transition and stable stages is very small and tends to be flat. It may happen because latent heat is more dominant than sensible heat. In the dry-out stage, the TR is increased because of the high temperature retards the motion of working fluid inside the OHP channel. Overall, the trend of thermal resistance decreases with the increase of heat supply.

Each stage has a different characteristic of the decrement of thermal resistance.
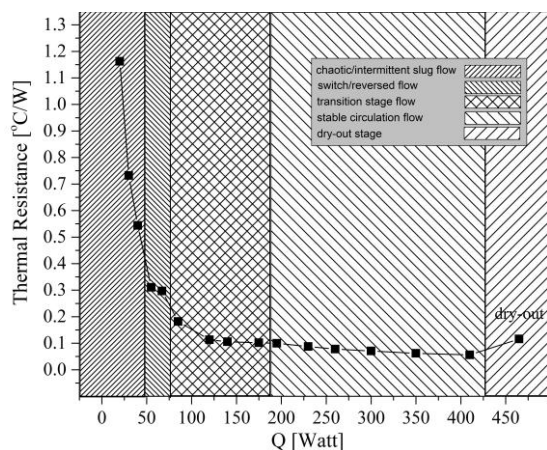

Fig. 9. Thermal Resistance

V. CONCLUSION

This study investigated the characteristic of temperature evolutions as a function of heat supply in an OHP with large-scale dimension using methanol working fluid. The temperature evolution can be associated with flow pattern as follows: chaotic intermittent slug flow, switch and reversed flow, transition to annular flow and stable circulation and dry-out stage. In the chaotic intermittent slug flow, the motions of fluid in OHP were very unstable and intermittent and tended to chaotic, which resulted in poor thermal resistance. At the switch/reversed flow stage, the evaporator temperatures separated into some levels which was a proof of net circulation flow. This separation of evaporator temperature level indicated that at 55 Watts higher velocity of fluid motions was generated from a larger driving force. At the transition stage the thermal resistance only slightly increased due to transition of the flow pattern.

The initial critical power at 195 Watts started sustainable stable net circulations. The higher speed of vapor plugs at annular flow pattern resulted in a decrease of vapor growth generation time. There was a step increase of average temperatures of evaporator, adiabatic and condenser from heat supply increments at the evaporator to 400 Watts. The evaporator temperature (T3 and T4) soared to more than 150°C after a certain time period of 465 Watts heat supply. The lowest thermal resistance was 0.057 °C/W at 410 Watts.

ACKNOWLEDGMENT

REFERENCES

[1] H. Akachi, United States, 1990.

[2] B. Tong, T. Wong, and K. Ooi, "Closed-loop pulsating heat pipe," *Applied thermal engineering,* vol. 21, no. 18, pp. 1845-1862, 2001.

[3] H. Ma, *Oscillating heat pipes*. Springer, 2015.

[4] C.-Y. Tseng, K.-S. Yang, K.-H. Chien, M.-S. Jeng, and C.-C. Wang, "Investigation of the performance of pulsating heat pipe subject to uniform/alternating tube diameters," *Experimental Thermal and Fluid Science,* vol. 54, pp. 85-92, 2014.

[5] X. Cui, Y. Zhu, Z. Li, and S. Shun, "Combination study of operation characteristics and heat transfer mechanism for pulsating heat pipe," *Applied Thermal Engineering,* vol. 65, no. 1-2, pp. 394-402, 2014.

[6] X. Liu, Y. Chen, and M. Shi, "Dynamic performance analysis on start-up of closed-loop pulsating heat pipes (CLPHPs)," *International Journal of Thermal Sciences,* vol. 65, pp. 224-233, 2013.

[7] R. Naik, V. Varadarajan, G. Pundarika, and K. R. Narasimha, "Experimental investigation and performance evaluation of a closed loop pulsating heat pipe," 2013.

[8] B. Verma, V. Yadav, and K. K. Srivastava, "Experimental Study on Thermal Performance Of Pulsating Heat Pipe With Al_2O_3-Deionizedwater Nanofluid At Different Orientations," *Journal of Enhanced Heat Transfer,* vol. 20, no. 2, 2013.

[9] J. Xu, Y. Li, and T. Wong, "High speed flow visualization of a closed loop pulsating heat pipe," *International Journal of Heat and Mass Transfer,* vol. 48, no. 16, pp. 3338-3351, 2005.

[10] M. Saha, C. Feroz, F. Ahmed, and T. Mujib, "Thermal performance of an open loop closed end pulsating heat pipe," *Heat and mass transfer,* vol. 48, no. 2, pp. 259-265, 2012.

[11] S. Lips, A. Bensalem, Y. Bertin, V. Ayel, C. Romestant, and J. Bonjour, "Experimental evidences of distinct heat transfer regimes in pulsating heat pipes (PHP)," *Applied Thermal Engineering,* vol. 30, no. 8-9, pp. 900-907, 2010.

[12] R. Borkar and P. Pachghare, "Thermo-Hydrodynamic Behavior of Methanol Charged Closed Loop Pulsating Heat Pipe," *Frontiers in Heat Pipes (FHP),* vol. 5, no. 1, 2014.

[13] H. R. Goshayeshi and I. Chaer, "Experimental study and flow visualization of Fe2O3/kerosene in glass oscillating heat pipes," *Applied Thermal Engineering,* vol. 103, pp. 1213-1218, 2016.

[14] H. Xian, W. Xu, Y. Zhang, X. Du, and Y. Yang, "Thermal characteristics and flow patterns of oscillating heat pipe with pulse heating," *International Journal of Heat and Mass Transfer,* vol. 79, pp. 332-341, 2014.

[15] V. Karthikeyan, K. Ramachandran, B. Pillai, and A. B. Solomon, "Understanding thermo-fluidic characteristics of a glass tube closed loop pulsating heat pipe: flow patterns and fluid oscillations," *Heat and Mass Transfer,* vol. 51, no. 12, pp. 1669-1680, 2015.

[16] P. Kiedcharoensiri, P. Charoensawan, and P. Terdtoon, "Two-Phase Flow Analysis of a Horizontal Closed-Loop Oscillating Heat Pipe," *Journal of Science and Technology MSU,* vol. 31, no. 5, pp. 571-577, 2012.

[17] S. Khandekar and M. Groll, "An insight into thermo-hydrodynamic coupling in closed loop pulsating heat pipes," *International journal of thermal sciences,* vol. 43, no. 1, pp. 13-20, 2004.

[18] M. Arab, M. Soltanieh, and M. Shafii, "Experimental investigation of extra-long pulsating heat pipe application in solar water heaters," *Experimental thermal and fluid science,* vol. 42, pp. 6-15, 2012.

[19] H. Xian, Y. Yang, D. Liu, and X. Du, "Heat transfer characteristics of oscillating heat pipe with water and ethanol as working fluids," *Journal of Heat Transfer,* vol. 132, no. 12, p. 121501, 2010.

[20] N. Soponpongpipat, P. Sakulchangsatjaati, N. Kammuang-Lue, and P. Terdtoon, "Investigation of the startup condition of a closed-loop oscillating heat pipe," *Heat Transfer Engineering,* vol. 30, no. 8, pp. 626-642, 2009.

[21] M. Mameli, M. Marengo, and S. Khandekar, "Local heat transfer measurement and thermo-fluid characterization of a pulsating heat pipe," *International journal of thermal sciences,* vol. 75, pp. 140-152, 2014.

[22] R. Senjaya and T. Inoue, "Oscillating heat pipe simulation considering dryout phenomena," *Heat and Mass Transfer,* vol. 50, no. 10, pp. 1429-1441, 2014.

[23] J. Li and L. Yan, "Experimental research on heat transfer of pulsating heat pipe," *Journal of thermal Science,* vol. 17, no. 2, pp. 181-185, 2008.

[24] W. Guoyou, Z. Nannan, J. Yulong, and H. Ma, "Velocity effect on liquid plug length in a capillary tube," *Journal of Heat Transfer,* vol. 135, no. 8, p. 080903, 2013.